

# Impact of Carrier Frequency Jitter on the Performance of Coherent Optical Systems with High-Order Modulation Formats

R. Bravo<sup>\*/\*\*\*</sup>, J. D. Reis<sup>\*\*</sup>, D. A. A. Mello<sup>\*\*\*</sup>

<sup>\*</sup>BrPhotonics Ltda., Campinas, Brazil

<sup>\*\*</sup>Idea! Electronic Systems, Campinas, Brazil

<sup>\*\*\*</sup>Unicamp, Campinas, Brazil

e-mail: r163653@dac.unicamp.br

**Abstract** - We investigate the impact of optical carrier frequency jitter on digital signal processing algorithms for coherent optical systems with high-order modulation formats. The jitter signal is modeled as a sinusoidal waveform and added to the optical carrier signal phase. Performance curves for QPSK, 16QAM and 64QAM are presented and OSNR penalties for a Pre-FEC limit of  $BER=2.4 \times 10^{-2}$  are obtained.

**Keywords:** Carrier frequency jitter, Coherent optical systems, Digital signal processing algorithms.

## 1 Introduction

Coherent detection enabled important benefits to high-speed optical communication systems. First, the implementation of high-order modulation formats strongly improves spectral efficiency. Second, the compensation of linear effects such as chromatic dispersion (CD) and polarization mode dispersion (PMD) simplifies the system operation and reduces capital and operational expenditures. The removal of CD compensating modules reduces the link insertion loss and improves the optical signal to noise ratio (OSNR) at the receiver side.

The performance of coherent optical systems may be severely impaired by transceiver imperfections, which have to be compensated by digital signal processing (DSP). Carrier phase and frequency effects are the most representative of these impairments. Carrier phase noise appears because of the non-monochromatic nature of the employed lasers, and carrier frequency offset is generated by differences in the operating frequencies of transmitter and local oscillator lasers. This frequency offset varies over time, as a result of inevitable mechanical vibrations that modify the laser oscillation frequency, a phenomenon known as carrier frequency jitter (CFJ). CFJ can significantly degrade the system performance, as demonstrated in [1].

CFJ has been evaluated in several previous publications [1–5], however, its impact on certain high-order modulation formats, e.g. 64 quadrature amplitude modulation (64QAM), has not been deter-

mined. Although the problem of carrier frequency recovery can be modeled analytically in certain conditions, its performance in practical systems depends strongly on the deployed signal processing algorithms. Therefore, this paper evaluates the impact of CFJ on system performance considering typical frequency and phase recovery algorithms. In particular, we investigate the following operating conditions: QPSK at 32 GBd (100 Gb/s), 16QAM at 32 GBd (200 Gb/s), 64QAM at 43 GBd (400 Gb/s) and 64 GBd (600 Gb/s). The system performance is assessed in terms of the optical signal to noise ratio (OSNR) required to achieve a  $BER=2.4 \times 10^{-2}$ .

## 2 System Setup

In an intradyne coherent receiver, a frequency offset  $\Delta_f$  is generated as a consequence of the difference between the operating frequencies of the transmitter and local oscillator lasers. This phenomenon needs to be properly controlled, since it is another source of perturbation on the received symbol phases [6, 7].

The phase deviation caused by a frequency offset changes slowly over time, being almost constant between adjacent symbols. Thus, the received signal in presence of phase noise and frequency offset is given by:

$$r_k = s_k e^{j(\theta_k + k\Delta_\Phi)} + w_k, \quad (1)$$

where  $s_k$  is the transmitted signal,  $\theta_k$  is the phase noise and  $w_k$  is the additive white Gaussian noise (AWGN) generated in optical amplifiers.  $\Delta_\Phi$  is the phase offset induced by the frequency offset  $\Delta_f$ , between instants  $k$  and  $k + 1$ :

$$\Delta_\Phi = 2\pi\Delta_f T_{sa}, \quad (2)$$

in which  $T_{sa}$  is the time between samples.

In practice,  $\Delta_f$  varies over time. References [8, 9] present a complete characterization of different types of digital jitter. In this work,  $\Delta_f$  is modeled

as sinusoidal process [10]:

$$\Delta_f(t) = \Delta_{F_1} + \frac{\Delta_A}{2} \sin(2\pi ft), \quad (3)$$

where  $\Delta_{F_1}$  is the average frequency offset between the two lasers and  $\Delta_A$  and  $f$  the peak-to-peak amplitude and the frequency variation of the sinusoidal jitter, respectively [5]. Frequency offsets are usually compensated by digital carrier recovery using non-data-aided techniques, such as the Mth-power algorithm [11].

In addition to CFJ, the non-monochromatic nature of lasers generates phase noise, rotating the received constellations. Phase noise can be modeled as a Wiener process, where the phase difference between consecutive symbols is a Gaussian random variable [12]. In this way, the phase shift  $\theta_k$  experienced by the  $k^{\text{th}}$  symbol is given by [13]:

$$\theta_k = \theta_{k-1} + \Delta_k = \sum_{m=0}^{k-1} \Delta_m, \quad (4)$$

where  $\Delta_k$  and  $\Delta_m$  are zero mean Gaussian-distributed random variables. Their variance  $\sigma_{\Delta}^2$  is given by:

$$\sigma_{\Delta}^2 = 2\pi\Delta_{\nu}T_{sa}, \quad (5)$$

where  $\Delta_{\nu}$  is the sum of the transmitter laser and local oscillator laser linewidths, and  $T_{sa}$  is the time between samples. Carrier phase recovery for higher-order QAM signals is commonly carried out by the Blind Phase Search (BPS) algorithm [13–15].

### 3 Simulation Setup

We investigated the four representative operating conditions depicted in Table 1. Additive and phase noise have been considered in all simulations.

Table 1 – Investigated Scenarios

Modulation Format	Symbol Rate (GBd)	Frequency Recovery Algorithm	Phase Recovery Algorithm
QPSK	32	Mth-power in frequency domain	BPS
16QAM	32		With
64QAM	43		N=100
	64		I=30

Transmitter and local oscillator carrier signals have been simulated according to:

$$S_k^{Tx} = Ae^{j\{[2\pi(\frac{\Delta_A}{2}\sin(2\pi f_A k T_{sa}))]kT_{sa} + \theta_k^{Tx}\}}, \quad (6)$$

$$S_k^{LO} = Ae^{j\{[2\pi(\Delta_{F_1} + \frac{\Delta_A}{2}\sin(2\pi f_A k T_{sa} + \phi))]kT_{sa} + \theta_k^{LO}\}}, \quad (7)$$

where  $\theta_k$  is the Wiener-distributed phase noise corresponding to a linewidth of 100 kHz,  $\Delta_{F_1}$  is the frequency offset, set to 1 GHz, and  $\phi$  is the phase shift between transmitter and local oscillator jitters, set to  $\pi$  as a worst-case condition. Parameters  $\Delta_A$  and  $f_A$  are the CFJ amplitude and frequency. Both values were configured in agreement with Table 2, which contains representative values used by component manufacturers.

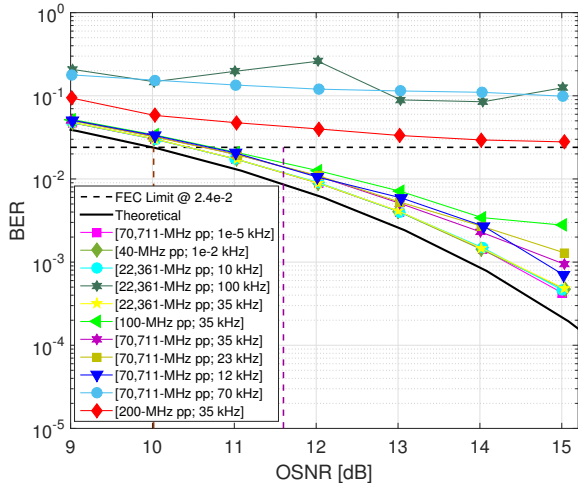
Table 2 – Parameter setup for CFJ

Index	Peak-to-Peak [MHz]	Frequency [kHz]
1	70,71	0,00001
2	40	0,01
3	22,36	10
4	22,36	100
5	22,36	35
6	100	35
7	70,71	35
8	70,71	23
9	70,71	12
10	70,71	70
11	200	35

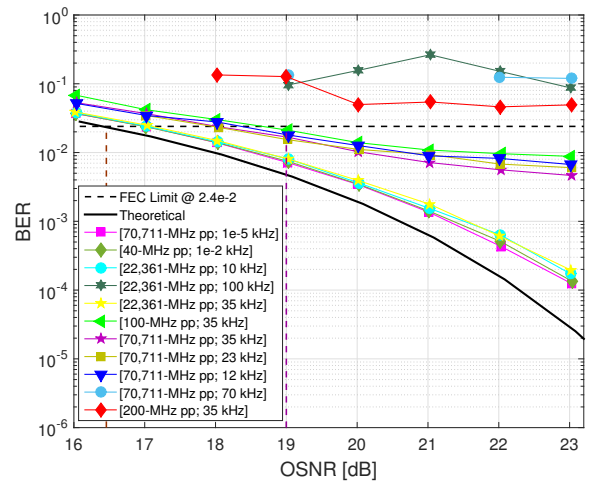
## 4 Results

Fig. 1 shows the performance achieved by the four simulated operating conditions. There are twelve curves in each figure: the black solid curve indicates the theoretical performance, while the others correspond to the CFJ scenarios presented in Table 2. The brown vertical dashed line indicates the theoretical OSNR required for the Pre-FEC BER limit of  $2.4 \cdot 10^{-2}$ , while the purple one corresponds to the maximum acceptable required OSNR suggested by manufacturers [16]. OSNR penalty values are calculated with respect to the Pre-FEC BER of  $2.4 \cdot 10^{-2}$  subtracting the theoretical OSNR to the simulated OSNR at this point for each curve.

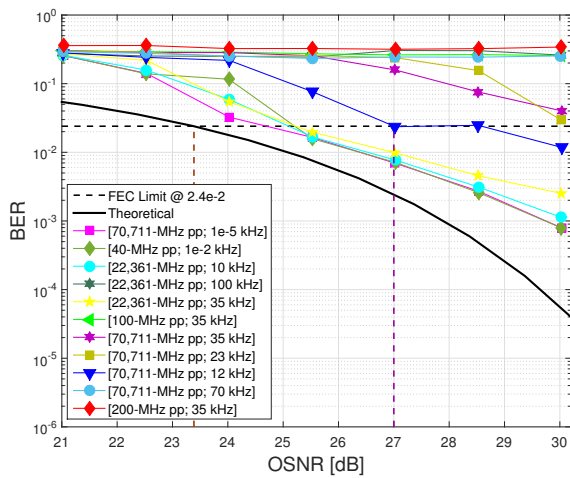
Fig. 1(a) shows the results for QPSK modulation at 32 GBd. Three of the eleven cases exhibit OSNR penalties exceeding the OSNR limit threshold. These cases correspond to CFJ configurations with a large peak-to-peak amplitude, a high oscillation frequency, and both conditions. It is interesting to observe that a low frequency can compensate a large peak-to-peak amplitude. This is the case of a CFJ with 100 MHz amplitude and 35-kHz frequency. Unlike, a high CFJ frequency cannot be easily compensated by a low amplitude, as evidenced in the curve of 22.36-MHz amplitude and 100-kHz frequency. The simulated performance was very similar for the remaining eight cases, with penalties ranging between 0.48 and 0.73 dB.



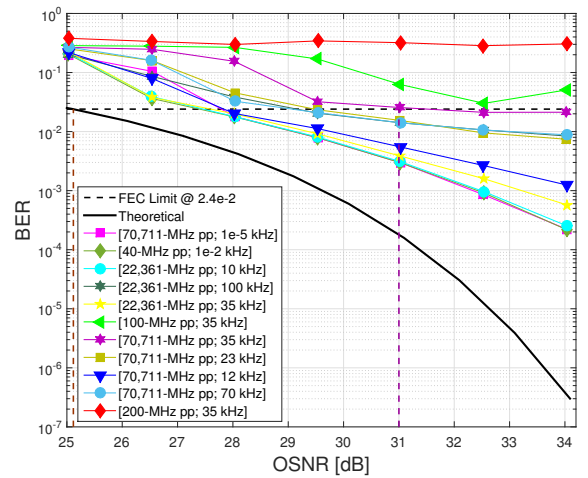
(a) QPSK at 32 GBd



(b) 16QAM at 32 GBd



(c) 64QAM at 43 GBd



(d) 64QAM at 64 GBd

Figure 1 – System performance with noise loading for the four simulated scenarios

A similar behavior was observed for 16QAM modulation at 32 GBd, and the minimum required performance was not achieved for the same three cases. For the other eight cases, although the performance degraded with respect to QPSK, the curves still attained the Pre-FEC limit in the allowed region, with penalties in the range between 0.54 to 2.24 dB.

Increasing the symbol rate and the modulation order severely degraded the system performance, as it can be observed in Figs. 1(c) and 1(d). Although an increase in symbol rate alleviates phase distortions because of shorter sampling times, raising the order of the modulation format degrades the system performance due to a small Euclidean distance between constellation points. For 64QAM at 43 GBd, only four of the eleven simulated scenarios achieved the recommended OSNRs. As expected, 64QAM at 64 GBd is less susceptible to

CFJ, and eight cases exhibited satisfactory performance.

Table 3 summarizes the OSNR penalties obtained for each case. The hyphen indicates scenarios for which the BER limit was not achieved, while the cells in red indicate the cases where the OSNR penalties remained outside the region determined by the vertical bars.

As expected, the CFJ impact is more prominent for high-order modulation formats, which inherently have a smaller phase noise tolerance due to the lower spacing between adjacent constellation points. On the other hand, for the same modulation format, the higher symbol rate improved the system robustness against phase noise, due to the proportional relation between phase offset and symbol period. It is interesting to observe that cases 4 and 10, which exhibit the highest CFJ frequency (100 and 70 kHz, respectively), could not

Table 3 – OSNR penalties

CFJ	PENALTY [dB] AT BER=2.4e-2			
	QPSK	16QAM	64QAM at 43GBd	64QAM at 64GBd
1	0,4834	0,5628	1,4369	2,8190
2	0,4936	0,5425	2,0158	2,4080
3	0,4841	0,5766	1,8852	2,4840
4	-	-	-	4,1230
5	0,4967	0,6721	1,9538	2,5760
6	0,7682	2,2471	-	-
7	0,6771	1,5594	-	6,4320
8	0,6627	1,5180	-	4,3710
9	0,7357	1,9536	4,1816	2,8110
10	-	-	-	4,0240
11	-	-	-	-

be recovered with a QPSK constellation at 32 GBd, but were recovered with a 64QAM constellation at 64 GBd. However, case 6, which has the highest CFJ amplitude (100 MHz), was recovered for QPSK at 32 GBd, but not for 64QAM at 64 GBd. This indicates an improved robustness against CFJ frequency in higher rates and modulation orders, but some susceptibility to the CFJ amplitude.

## Conclusions

In this paper we investigated the system impact of CFJ modeled as a sinusoidal perturbation. We evaluated OSNR penalties with respect to a pre-FEC BER=2.4×10<sup>-2</sup> for four representative transmission conditions and eleven CFJ levels. Increasing the bit rate of optical transceivers can be accomplished by raising the symbol rate, or the order of the modulation format. While raising the symbol rate strongly improves robustness against the CFJ frequency rate, increasing the order of the modulation format can lead to a higher vulnerability to CFJ amplitude variation.

## Acknowledgements

This work was supported by BrPhotonics.

## References

- [1] K. Piyawanno et al., “Effects of mechanical disturbance on local oscillators and carrier synchronization,” in *OECC 2010 Technical Digest*, pp. 124–125, July 2010.
- [2] M. Qiu et al., “Simple and efficient frequency offset tracking and carrier phase recovery algorithms in single carrier transmission systems,” *Opt. Express*, vol. 21, pp. 8157–8165, Apr 2013.
- [3] P. Gianni et al., “A new parallel carrier recovery architecture for intradyne coherent optical receivers in the presence of laser frequency fluctuations,” in *2011 IEEE Global Telecommunications Conference - GLOBECOM 2011*, pp. 1–6, Dec 2011.
- [4] P. Gianni et al., “Compensation of laser frequency fluctuations and phase noise in 16-QAM coherent receivers,” *IEEE Photonics Technology Letters*, vol. 25, pp. 442–445, March 2013.
- [5] M. Kuschnerov et al., “Impact of mechanical vibrations on laser stability and carrier phase estimation in coherent receivers,” *IEEE Photonics Technology Letters*, vol. 22, pp. 1114–1116, Aug 2010.
- [6] M. Selmi et al., “Accurate digital frequency offset estimator for coherent PolMux QAM transmission systems,” in *2009 35th European Conference on Optical Communication*, pp. 1–2, Sept 2009.
- [7] S. Hoffmann et al., “Frequency and phase estimation for coherent QPSK transmission with unlocked DFB lasers,” *IEEE Photonics Technology Letters*, vol. 20, pp. 1569–1571, Sept 2008.
- [8] S. Sunter et al., “On-chip digital jitter measurement, from megahertz to gigahertz,” *IEEE Design Test of Computers*, vol. 21, pp. 314–321, July 2004.
- [9] N. Ou et al., “Jitter models for the design and test of Gbps-speed serial interconnects,” *IEEE Design Test of Computers*, vol. 21, pp. 302–313, July 2004.
- [10] R. M. da Silva Ferreira, *Advanced Digital Signal Processing for Flexible Optical Access Networks*. PhD thesis, University of Aveiro, Portugal, 2017.
- [11] M. S. Faruk et al., “Digital signal processing for coherent transceivers employing multilevel formats,” *Journal of Lightwave Technology*, vol. 35, pp. 1125–1141, Mar 2017.
- [12] P. Mathecken et al., “Performance analysis of OFDM with wiener phase noise and frequency selective fading channel,” *IEEE Transactions on Communications*, vol. 59, pp. 1321–1331, May 2011.
- [13] T. Pfau et al., “Hardware-efficient coherent digital receiver concept with feedforward carrier recovery for M-QAM constellations,” *Journal of Lightwave Technology*, vol. 27, pp. 989–999, April 2009.
- [14] J. Li et al., “Laser-linewidth-tolerant feed-forward carrier phase estimator with reduced complexity for QAM,” *Journal of Lightwave Technology*, vol. 29, pp. 2358–2364, Aug 2011.
- [15] X. Zhou et al., “Modulation-format-independent blind phase search algorithm for coherent optical square m-qam systems,” *Opt. Express*, vol. 22, pp. 24044–24054, Oct 2014.
- [16] J. D. Reis et al., “Technology options for 400G implementation,” tech. rep., Optical Internetworking Forum, 2015.